Insertion of the Al Atom into the NH_3 Molecule: Semiempirical SCF MO and Matrix Isolation ESR Study

Paul H. Kasai[†] and Hans-Jörg Himmel[‡]

IBM Research Division, Almaden Research Center, 650 Harry Road, San Jose, California 95120-6099, and Institut für Anorganische Chemie der Universität Karlsruhe (TH), Engesserstrasse, 76128 Karlsruhe, Germany

Received: March 6, 2002; In Final Form: May 17, 2002

The insertion process of the Al atom into the ammonia molecule (NH_3) was examined by a semiempirical SCF molecular orbital method (AM1) and by matrix isolation ESR spectroscopy. The MO study revealed the three-step process: (1) the spontaneous formation of the dative complex Al:NH_3 driven by the three-electron bonding scheme between the unpaired electron of Al and the lone pair electrons of NH_3, (2) cleavage of a N−H bond upon vibrational excitation of the Al:NH_3 complex, and (3) completion of the insertion process by the three-electron bonding scheme between the unpaired electron on the cleaved hydrogen atom and the lone pair electrons on Al. The ESR study revealed the spontaneous formation of the dative complex Al:NH_3 upon co-condensation of Al atoms and NH_3 in argon matrixes, and its conversion to the insertion radical H−Al−NH_2 when the matrix was irradiated with near-IR light ($\lambda = 700 \pm 50$ nm). In matrixes with higher NH_3 concentration ($\geq$2%), the insertion radical complexed with the second NH_3 molecule, (H−Al−NH_2):NH_3, was also formed. Irradiation of matrixes containing these insertion radicals with blue light ($\lambda = 450 \pm 50$ nm) effected the dissociation processes H−Al−NH_2 → H• + Al−NH_2 and (H−Al−NH_2):NH_3 → 2H• + Al$(NH_2)_2$. Well-resolved ESR spectra assigned to the dative complex Al:NH_3, the insertion radical H−Al−NH_2, its complex (H−Al−NH_2):NH_3, and the diligand species Al$(NH_2)_2$ were observed, analyzed, and discussed.

Introduction

Many matrix isolation studies have shown that the Al atom has a propensity to insert itself into heteroatomic bonds. Hauge et al., using the matrix isolation IR method, observed spontaneous formation of H−Al−OH upon co-condensation of Al atoms and H_2O in argon matrixes.[1] Knight et al. observed and analyzed later the ESR spectra of H−Al−OH generated in neon and argon matrixes.[2] Howard et al. reported on an ESR study of the corresponding insertion product H−Al−NH_2 upon co-condensation of Al atoms and NH_3 in adamantane matrixes at 77 K.[3] Chenier et al. reported on the ESR spectra of insertion products R−Al−O−R generated upon co-condensation of Al atoms and various alkyl ethers in adamantane matrixes.[4] More recently a matrix isolation ESR study at one of our laboratories revealed formation of H−Al−Cl upon co-condensation of Al atoms and HCl molecules in argon matrixes.[5] In each of these papers, on the basis of the fact that the reaction occurred in a cryogenic environment, it was asserted that Al atoms in the ground state reacted spontaneously to form the observed insertion radicals. Himmel et al., on the other hand, examined the reaction between group III atoms (Al, Ga, and In) and NH_3 co-condensed in argon matrixes by IR and UV−vis spectroscopy and observed spontaneous formation of the dative complex M:NH_3 (M = Al, Ga, In) and its conversion to the insertion product H−M−NH_2 upon irradiation of the matrix at $\lambda = 436$ nm.[6] Himmel et al. further found that the resulting insertion radical was photolabile and decomposed to yield M−NH_2 when the matrix was irradiated with broad UV−vis light ($200 \leq \lambda \leq 800$ nm).[6] A more definitive study of the reaction process between Al and NH_3 leading to the insertion radical appears warranted.

Most recently the reaction between Al atoms and dimethyl ether (DME) was examined at one of our laboratories.[7] The most plausible reaction passage was examined by a semiempirical SCF method (AM1) and by the matrix isolation ESR technique. The molecular orbital study revealed that the insertion product CH_3−Al−O−CH_3 would be formed in three steps: (1) spontaneous formation of the dative complex Al:O$(CH_3)_2$ driven by a flow of the unpaired electron of the Al atom into the LUMO (lowest unoccupied molecular orbital) of the DME system, (2) cleavage of one of the CH_3−O bonds, and (3) completion of the insertion process driven by the three-electron reaction scheme between the unpaired electron on the CH_3 radical and the lone pair electrons on the Al atom. The theory predicted the presence of a small barrier (~8 kcal/mol) between the stationary state of the dative complex Al:O$(CH_3)_2$ and the onset of the methyl radical cleavage.[7]

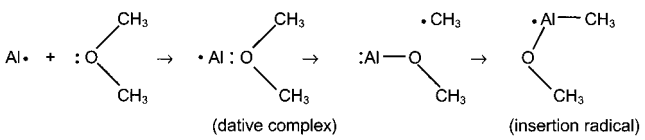

Examination of the matrixes in which Al atoms and DME were co-condensed showed the presence of both the dative

[†] Almaden Research Center.
[‡] Institut für Anorganische Chemie der Universität Karlsruhe (TH).

10.1021/jp0206424 CCC: $22.00
Published on Web 06/27/2002

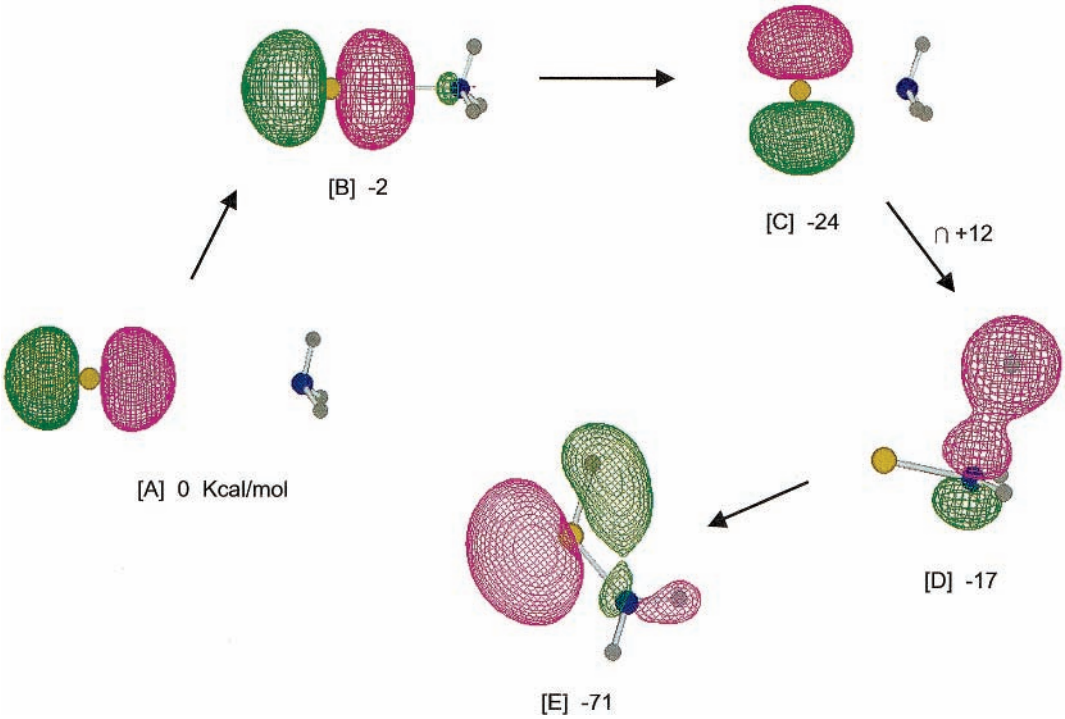

Figure 1. Insertion process of the Al atom into the NH_3 molecule revealed by the SCF MO (AM1) method. The energy level (relative to the starting separated system) and the isosurface contour rendering of the SOMO at each stage are shown.

complex and the insertion radical. Irradiation of the matrix with near-IR light ($\lambda = 700 \pm 50$ nm) resulted in the disappearance of the dative complex and corresponding increase of the insertion radical. The near-IR irradiation is believed to excite the dative complex vibrationally and initiate the insertion process.

We have now examined the reaction between Al and NH_3 similarly first by the semiempirical SCF MO method, followed by the matrix isolation ESR spectroscopy. In this paper we report on the results thence obtained. It was anticipated that the insertion of Al into NH_3 would also occur in three steps: (1) a spontaneous formation of the dative complex Al:NH_3, (2) cleavage of one of the N−H bonds, and (3) completion of the process driven by the three-electron bonding scheme between the unpaired electron of the cleaved hydrogen and the lone pair electrons on the Al atom.

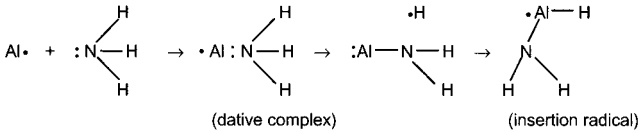

This was indeed found to be the case. In complete analogy to the steps found in the Al−DME case, the dative complex was formed spontaneously, and the insertion process commenced upon irradiation with near-IR light ($\lambda = 700 \pm 50$ nm). A subtle difference was found in the electronic symmetry of the dative complex (the E state as opposed to the A_1 state found for Al:DME). It was also found that the insertion radical underwent the photolysis process H−Al−NH_2 → H• + Al−NH_2 upon irradiation with blue light ($\lambda = 450 \pm 50$ nm).

Most interestingly, in matrixes with higher NH_3 concentration (≥2%), the insertion radical complexed with the second NH_3 molecule, (H−Al−NH_2):NH_3, was formed. This radical, when irradiated with blue light ($\lambda = 450 \pm 50$ nm), decomposed as follows: (H−Al−NH_2):NH_3 → 2H• + Al(NH_2)$_2$.

Experimental and Computational Methods

A liquid helium cryostat that would allow trapping of vaporized metal atoms in an argon matrix and examination of the resulting matrix by ESR has been described previously.[8] In the present series of experiments, Al atoms were vaporized from a resistively heated (~1400 °C) tantalum tube and were trapped in argon matrixes containing NH_3 (1−3%). All the ESR spectra were obtained while the matrix was maintained at ~4 K. The spectrometer frequency locked to the sample cavity was 9.428 GHz. For photoirradiation of the resulting matrix a high-pressure Xe/Hg lamp (Oriel, 1 kW) fitted with a water filter and a broadband interference filter of appropriate choice was used. NH_3 was obtained from Aldrich Chemical Co., and $^{15}ND_3$ (enrichment ≅98% for both ^{15}N and D) was obtained from Cambridge Isotope Laboratories, Inc.

For examination of the viable reaction passage by the semiempirical SCF molecular orbital method, the AM1 program implemented in HyperChem was used.[9] The NH_3 molecule was first geometry optimized, and the Al atom was placed ~3 Å away; the total system was then geometry optimized following the energy surface trough. For simulation of ESR spectra a Fortran program written and described earlier[10] was modified for execution on an IBM-compatible PC using the Absoft compiler.[11]

Computational Results

Examination of the reaction between the Al atom and NH_3 by the SCF semiempirical molecular orbital method (AM1), in

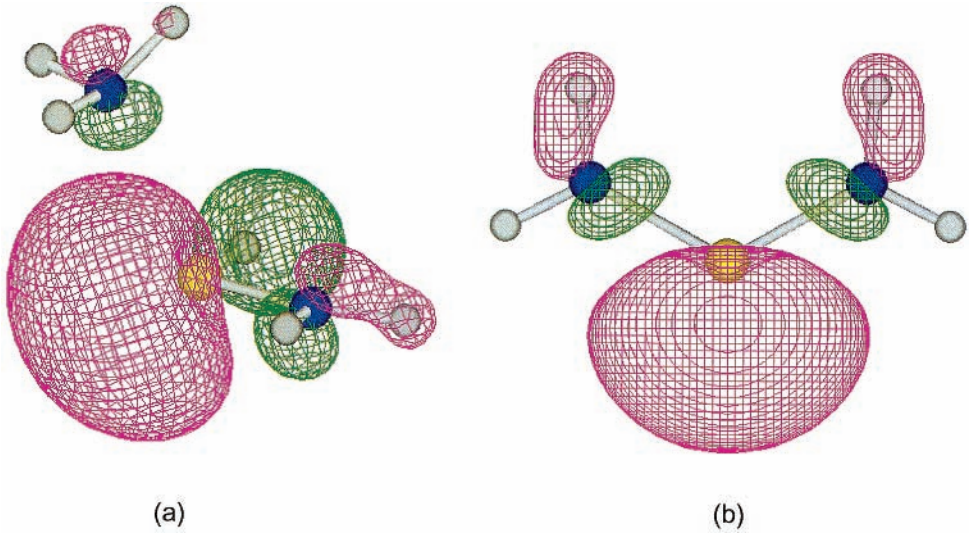

Figure 2. Structure and isosurface contour rendering of the SOMO of (a) the complexed insertion radical $(H-Al-NH_2):NH_3$ and (b) the diligand species $Al(NH_2)_2$.

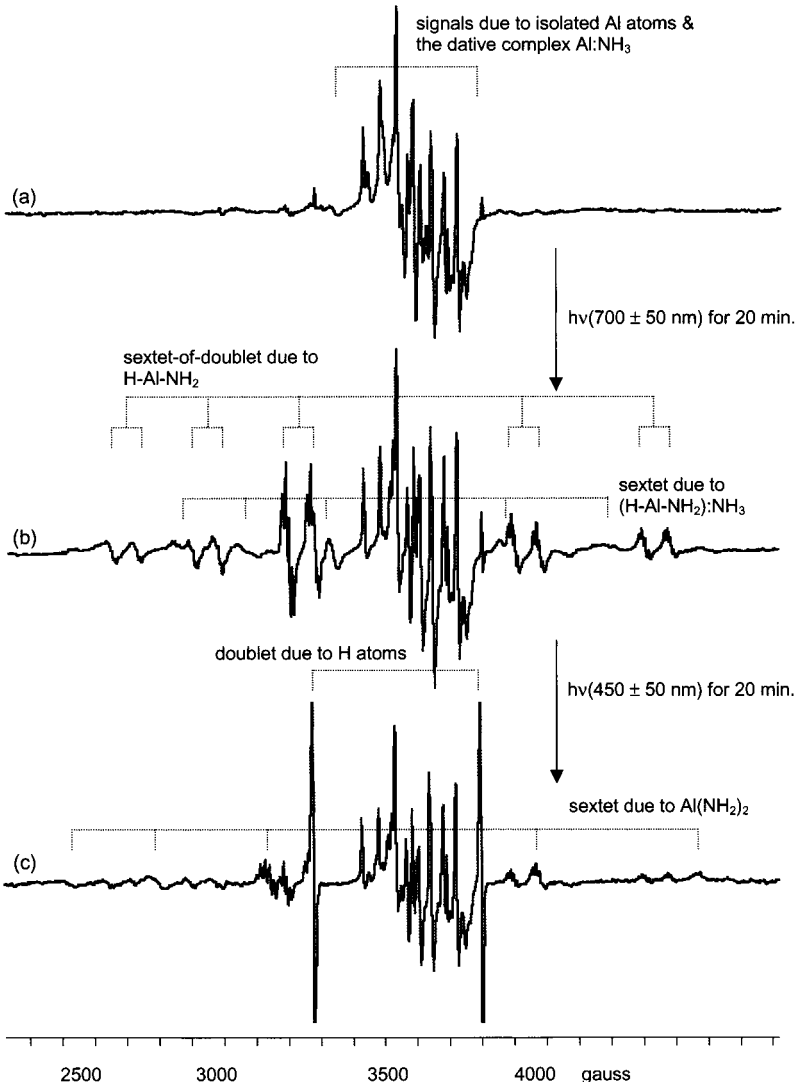

Figure 3. ESR spectra observed from the Al/NH_3 (1%)/argon system (a) as prepared, (b) after irradiation with near-IR light ($\lambda = 700 \pm 50$ nm) for 20 min, and (c) after subsequent irradiation with blue light ($\lambda = 450 \pm 50$ nm) for 20 min.

a manner completely analogous to that performed for the Al−DME system,[7] revealed the reaction passage depicted in Figure 1. For each stage the energy level relative to the starting separated system, the positions of the atoms, the bonds, and the isosurface contour rendering of the SOMO (singly occupied molecular orbital) are shown. It is revealed that the Al atom

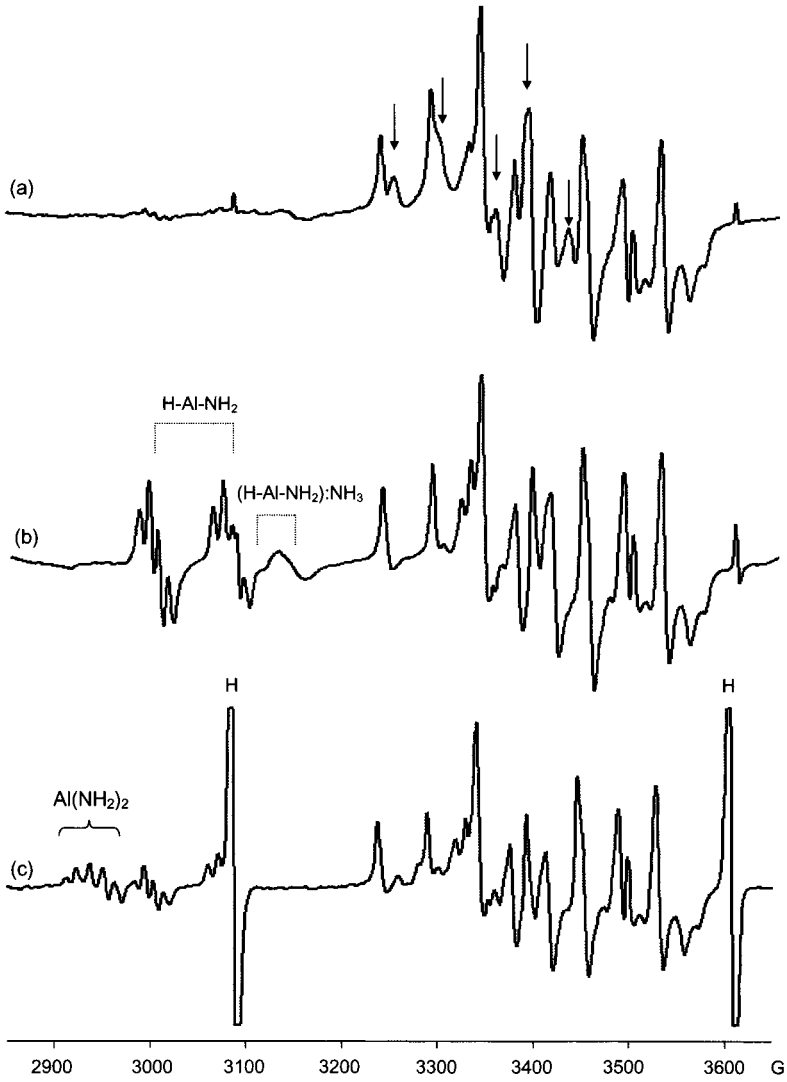

Figure 4. ESR spectra obtained from the same matrix as in Figure 3 scanning the central range: (a) as prepared, (b) after irradiation with near-IR light ($\lambda = 700 \pm 50$ nm) for 20 min, and (c) after subsequent irradiation with blue light ($\lambda = 450 \pm 50$ nm) for 20 min. The arrows in (a) indicate the photolabile signals due to the dative complex Al:NH_3.

approaches the nitrogen atom along the C_{3v} symmetry axis of the molecule driven by the three-electron bonding scheme between the unpaired electron of the Al atom and the lone pair electrons of the nitrogen atom. The unpaired electron thus initially resides in the orbital of A_1 symmetry given by the antibonding combination of the interacting orbitals (stage B in Figure 1). When the Al−N distance becomes ∼3 Å or less, however, the unpaired electron moves into the Al p orbital perpendicular to the Al−N internuclear direction. The degeneracy of the p_π orbitals is lifted by the Jahn−Teller effect. The reacting system then reaches a stationary state of a dative complex, Al:NH_3, at −24 kcal/mol (stage C). In the dative complex, the Al−N bond length is 2.3 Å and the Al atom bears a negative charge of −0.24, reflecting the dative interaction of the nitrogen's lone pair electrons into the Al valence orbitals. At this stage in the calculation, if the nitrogen atom is moved slightly upward (∼0.1 Å), *mimicking the asymmetric N−H stretching vibration*, cleavage of a hydrogen atom commenced as indicated (stage D). The barrier height of ∼12 kcal/mol was noted for the process. The final insertion product (stage E) is now spontaneously formed driven by the three-electron bonding scheme between the hydrogen's unpaired electron and the lone pair electrons of the Al atom. A heat of the insertion process of −71 kcal/mol was thus predicted.

As mentioned earlier, the current experimental study revealed the formation of the insertion radical complexed with the second NH_3 molecule, (H−Al−NH_2):NH_3, and the diligand species Al-$(NH_2)_2$. Figure 2 shows the structures and SOMOs of these radicals given by the AM1 method. It is revealed that *the complexed insertion radical* (H−Al−NH_2):NH_3 is essentially the insertion radical with the second NH_3 molecule datively interacting with the vacant Al p orbital perpendicular to the molecular plane. The calculation yielded a heat of association (for the second NH_3) of 18.5 kcal/mol. The diligand complex is shown to be completely planar. Interestingly its SOMO indicates that the ESR spectrum of the complex may exhibit, in addition to the hfs (hyperfine structure) due to the Al and nitrogen nuclei, a further hfs due to two protons situated trans to the main spin density lobe.

Experimental Results

Figure 3 shows the ESR spectra of the Al/NH_3 (1%)/argon system observed (a) as prepared, (b) after irradiation with near-IR light ($\lambda = 700 \pm 50$ nm) for 20 min, and (c) after subsequent

irradiation with blue light ($\lambda = 450 \pm 50$ nm) for 20 min. Figure 4 shows the spectra obtained from the same matrix scanning, at each corresponding stage, only the central range (2850−3650 G) for closer inspection.

The ESR spectra of aluminum atoms isolated in rare gas matrixes had been analyzed by Ammeter et al.[12] The ESR spectrum of the otherwise degenerate system ($3s^2 3p^1$) becomes observable owing to an axially symmetric lattice distortion. The unpaired electron thus resides in the nondegenerate 3p orbital. The Al hfc (hyperfine coupling) tensor of $A_{||} = +47.7$ G and $A_{\perp} = -33.7$ G has been determined for Al atoms isolated in argon matrixes. According to the MO study presented above, the unpaired electron in the dative complex Al:NH_3 is also localized in an Al p orbital (cf. stage C in Figure 1). In the spectra of the as-prepared matrix (Figures 3a and 4a), most of the signals are confined in the central section (3200−3600 G, indicated by a bracket in Figure 3a). Most of these signals are due to isolated Al atoms. A closer examination of the spectrum revealed that several additional signals were present within the same range and these signals disappeared upon irradiation with near-IR light (indicated by arrows in Figure 4a). On the basis of the similarity of the pattern to that of the isolated Al atoms and the photolability, these signals were (tentatively) assigned to the dative complex Al:NH_3.

Most interestingly the near-IR irradiation resulted in the appearance of a sextet-of-doublets (with some partially resolved additional structures) and a broad sextet indicated in Figure 3b. The sextet-of-doublets pattern observed here is very similar to that observed by Howard et al. in an adamantane matrix at 77 K, and assigned to the insertion radical H−Al−NH_2.[3] The intensity of the broad sextet relative to the sextet-of-doublets was found to parallel the NH_3 concentration. The relative intensity doubled when the NH_3 concentration was doubled, and diminished to nil when the concentration was decreased to 0.5%. The large essentially isotropic sextet feature observed in either pattern must surely be the hf structure due to the ^{27}Al nucleus ($I = 5/2$), and indicates a substantial unpaired electron density in an sp-hybridized orbital of the Al atom. The sextet-of-doublets was thus assigned to the insertion radical H−Al−NH_2, and the broad sextet to the insertion radical complexed to the second NH_3 molecule, (H−Al−NH_2):NH_3.

Subsequent irradiation of the matrix with blue light ($\lambda = 450 \pm 50$ nm) caused the diminution (or disappearance) of signals due to both H−Al−NH_2 and (H−Al−NH_2):NH_3 and the appearance of an intense doublet due to hydrogen atoms and a new sextet of wider spacings (Figures 3c and 4c). Decomposition of H−Al−NH_2 and generation of isolated hydrogen atoms are consistent with the photolysis process H−Al−NH_2 → H• + Al−NH_2 observed earlier by Himmel et al.[6] As for the new sextet with a larger Al hfc interaction, on the basis of the result of IR analysis performed concurrently with this study[13] and the hf structure analysis of the ESR spectrum (vide infra), it was assigned to the diligand Al molecule Al$(NH_2)_2$. See Figure 2b. The amount of the diligand species generated was found to parallel the amount of *the complexed insertion radical* (H−Al−NH_2):NH_3 present prior to irradiation with blue light. It is strongly suggested that the diligand species is generated as follows: (H−Al−NH_2):NH_3 → 2H• + Al$(NH_2)_2$.

Analysis of the Spectrum due to Al:NH_3. As stated above the signals observed from the matrix in the central section (prior to irradiation) are due to isolated Al atoms and the dative complex Al:NH_3. To differentiate the two sets of signals, a matrix with a higher NH_3 concentration (3%) was prepared. Figure 5a shows the spectra observed from this matrix before (in blue color) and after (in red color) irradiation with near-IR light for 20 min. The central section (3200−3650 G) encompassing the higher field component of the hydrogen doublet is shown. The signals due to Al:NH_3 are seen in much greater intensity (relative to those of Al atoms), and their total disappearance after irradiation is conspicuously demonstrated. Figure 5b shows the result of subtracting the postirradiation spectrum from the initial spectrum. The signals observed after irradiation are those of isolated Al atoms and the fourth component of the insertion radicals. The contribution of the latter radicals in the overall appearance of the pattern in this sector was recognized to be minimal. The prominent features seen in Figure 5b were thus concluded to be those of the dative complex Al:NH_3; the signals indicated by arrows were recognized as those belonging to the lowest (or the highest) field pairs of the Al hf components of the **g** tensor of orthorhombic symmetry. The tensors thus determined are given in Table 1. Figure 5c shows the spectrum simulated on the basis of these tensors. The weak features seen in Figure 5b but not reproduced in the simulation are due to the photoinduced insertion radicals.

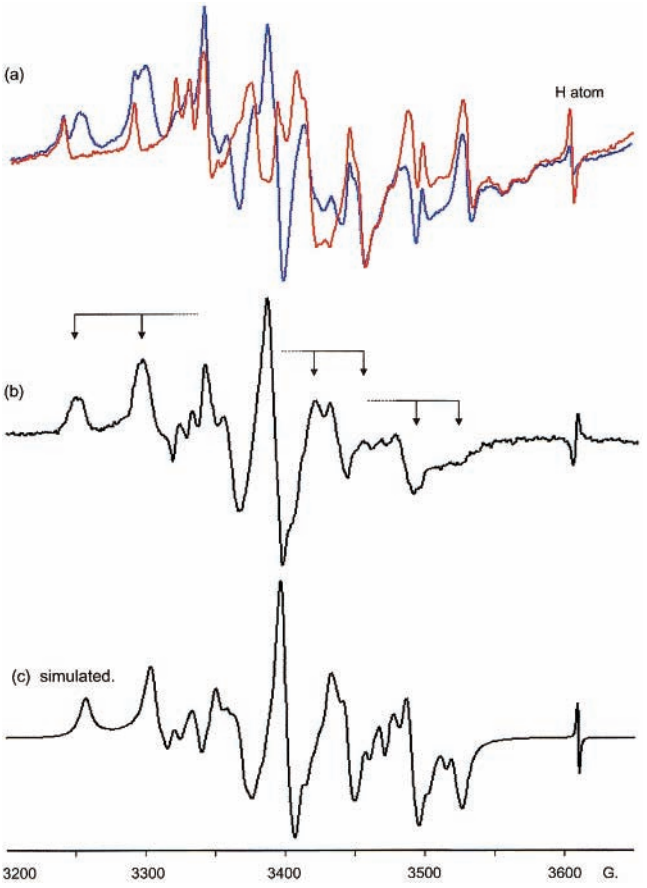

Figure 5. (a) ESR spectra observed from the Al/NH_3(3%)/argon system before (blue) and after (red) irradiation with near-IR light ($\lambda = 700 \pm 50$ nm) for 20 min. The central section (3200−3650 G) encompassing the high-field component of the hydrogen doublet is shown. (b) Spectrum obtained by subtracting the red from the blue in (a). The resultant pattern is attributed to the dative complex Al:NH_3 and is analyzed in terms of the **g** tensor and the Al hfc tensor of orthorhombic symmetry as indicated. (c) Simulated pattern based on the **g** tensor and the Al hfc tensor given in Table 1.

TABLE 1: g Tensors and Hyperfine Coupling Tensors Determined for Radicals Generated in the Al/NH_3 System

radical	**g** tensor ($g_\parallel/g_\perp/g_\perp$)	A(Al) (G) ($A_\parallel/\boldsymbol{A}_\perp/\boldsymbol{A}_\perp$)	$A(H_{H-Al})$ (G)	$A(^{14}N)$ (G)	$A(H_{NH_2})$ (G)
Al:NH_3	2.001/1.995/1.957	47/31/30			
H−Al−NH_2	2.002/2.002/1.999	376/321/321	76	9.5	9.5
(H−Al−NH_2):NH_3	2.000/2.000/1.996	305/265/265	34	∼10[a]	∼10[b]
Al(NH_2)$_2$	1.996/1.996/1.993	430/395/395		14.0	10.0

[a] Only the trans proton (relative to the spin density lobe) exhibits an observable hfc interaction. [b] Estimated from the overall line width.

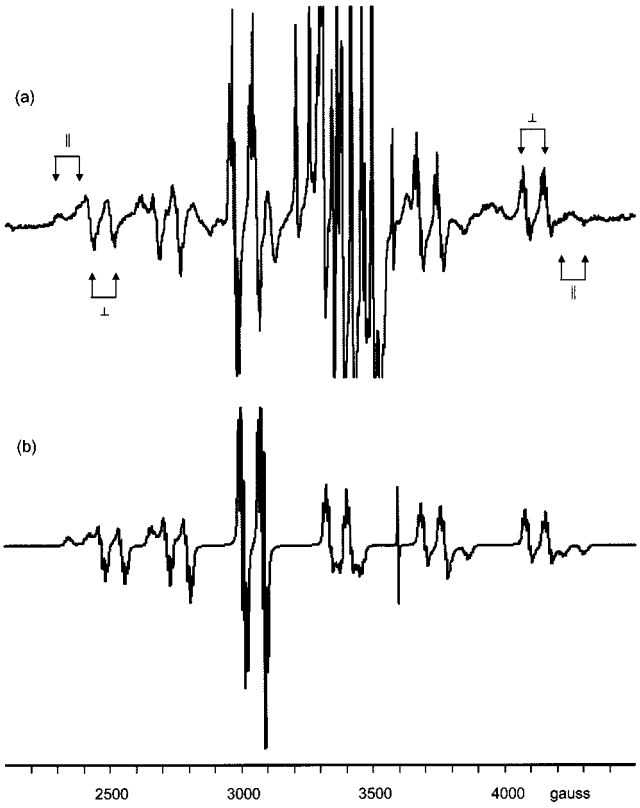

Figure 6. (a) ESR spectrum observed from the Al/NH_3 (1%)/argon system after irradiation with near-IR light (same as that in Figure 3b) shown in a vertically expanded scale. The sextet-of-doublets pattern assigned to the insertion radical H−Al−NH_2 clearly reveals the features due to an axially symmetric Al hfc tensor (indicated for the lowest and the highest field components). (b) Spectrum simulated on the basis of the **g** tensor and the hfc tensors given in Table 1. The doublet signals due to isolated hydrogen atoms are superposed for calibration.

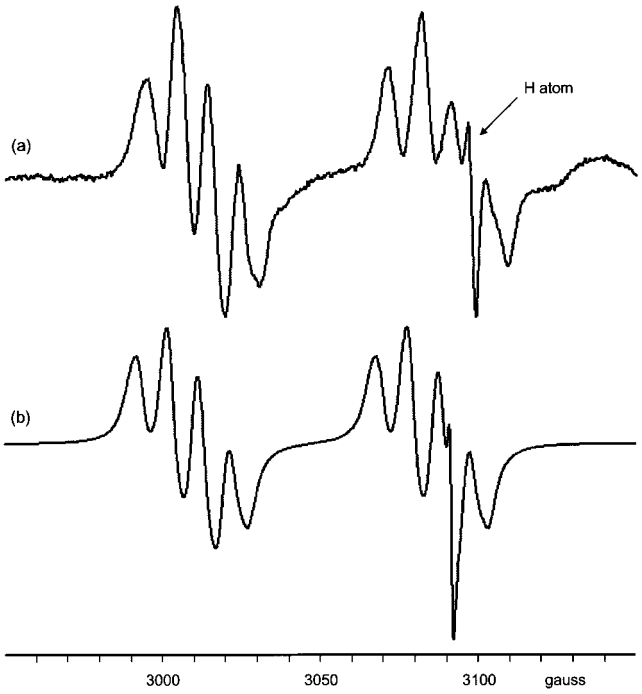

Figure 7. (a) Third Al hyperfine component of the insertion radical H−Al−NH_2 shown in an expanded scale. The doublet splitting is due to the H attached to the Al, and the quartet pattern is ascribed to the coupling to the ^{14}N nucleus and the coupling of (accidentally) the same magnitude to one of the amino protons. (b) Spectrum simulated on the basis of the tensors given in Table 1. The lower field component of the hydrogen atom doublet is superposed for calibration.

Analysis of the Spectrum due to H−Al−NH_2. The ESR spectrum of the Al/NH_3 (1%)/Ar system observed after irradiation with near-IR light ($\lambda = 700 \pm 50$ nm) is shown in Figure 6 in a vertically expanded scale. As stated earlier the Al hfc tensor of the insertion radical is large and essentially isotropic. A closer examination of the sextet-of-doublets pattern, however, clearly revealed the characteristics due to an axially symmetric hfc tensor as indicated for the lowest and the highest field components. The hfc interaction with the H attached to the Al is ∼80 G and is isotropic. Apparently, in this type of Al radical, the effect of the anisotropy of the Al hfc tensor vanishes for the third Al hf component ($m_I = 1/2$), hence the prominence of this component relative to the others. Figure 7a shows, in an expanded scale, the region encompassing this third Al hf component. It is seen that each component (of the doublet due to the H attached to Al) is further split into a quartet with successive spacings of ∼10 G. This pattern was observed by Howard et al. in their study of the radical generated in an adamantane matrix. They attributed this pattern to the hf interaction with the ^{14}N nucleus ($I = 1$), and the hf interaction of (accidentally) the same magnitude with one of the amino protons. It is illustrative to see the SOMO of the insertion radical shown in Figure 1 (stage E). Of the protons in the NH_2 sector, only the trans proton (relative to the main spin density lobe) has a significant unpaired electron density.

From the resonance positions of the highest and lowest field components ($m_I = \pm 5/2$) the **g** tensor and the Al hfc tensor of the insertion radical were determined as given in Table 1. For analysis of the ESR spectral pattern characterized by a large hfc tensor, the exact solution of the spin Hamiltonian based on the continued fraction technique was used.[14] The hfc tensor of the ^{14}N nucleus and that of the amino proton presently determined are also included in Table 1. Figures 6b and 7b show the spectra simulated on the basis of these tensors. In the simulated spectra, for the purpose of calibration, the signals due to isolated hydrogen atoms are superposed.

Spectra Observed from the Al/$^{15}ND_3$/Ar System. The spectral signals assigned to *the complexed insertion radical* (H−Al−NH_2):NH_3 in Figures 3 and 4 are broad and do not allow the assessment of the hfc constant of the H attached to the Al.

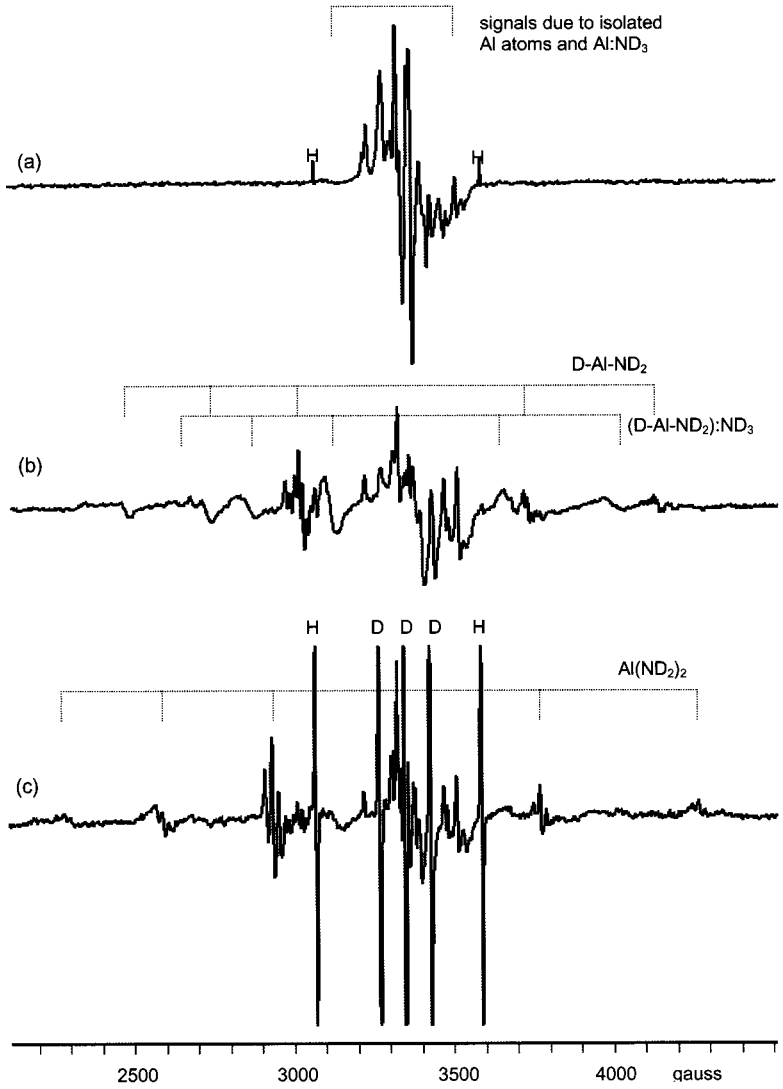

Figure 8. ESR spectra observed from the Al/$^{15}ND_3$ (2%)/argon system (a) as prepared, (b) after irradiation with near-IR light ($\lambda = 700 \pm 50$ nm) for 20 min, and (c) after subsequent irradiation with blue light ($\lambda = 450 \pm 50$ nm) for 20 min.

As for the signals assigned to the diligand species $Al(NH_2)_2$ in Figures 3 and 4, the multiplet structure resolved within each Al hf component indicates a multiplicity higher than that expected from the hfc interaction with two ^{14}N nuclei. To resolve these issues, the matrix experiment was performed using doubly isotopically enriched ammonia, $^{15}ND_3$. Figures 8 and 9 show the corresponding photolysis sequences thus observed from the Al/$^{15}ND_3$ (2%)/argon system. The dative complex Al:ND_3, the insertion radical D−Al−ND_2, *the complexed insertion radical* (D−Al−ND_2):ND_3, and the diligand species $Al(ND_2)_2$ were all recognized as indicated. The presence of the signals due to the dative complex Al:ND_3 and their disappearance upon irradiation with near-IR is clearly revealed in Figure 9. Parts a and b of Figure 10 show, in an expanded scale, the third Al hf component region of the spectra observed from the Al/NH_3/Ar and Al/^{15}-ND_3/Ar systems, respectively. The extra complexity of the D−Al−ND_2 component was ascribed to the presence of $^{15}ND_2H$ generated by an inadvertent back-exchange. Figure 10c shows the computed patterns of the insertion radicals D−Al−$^{15}ND_2$, D−Al−^{15}NHD, and H−Al−$^{15}ND_2$ (on the basis of the tensors given in Table 1 and making appropriate adjustments for the isotopic substitutions) for the assumed abundance ratio of 3/1/1. The computed patterns reveal that, if D−Al−^{15}NHD were present in a significant quantity, its signals would fill up the troughs of the quartet due to D−Al−$^{15}ND_2$. A strong isotope effect favoring the Al insertion into the N−H bond over the N−D bond is thus indicated.

Analysis of the Spectrum due to (H−Al−NH_2):NH_3. As stated above, the signals due to *the complexed insertion radical* comprise a broad sextet. The **g** tensor and the Al hfc tensor of the radical could be assessed, albeit with less accuracy, from the resonance positions indicated in Figure 3b or in Figure 8b. The broadness of the signals is surely due to the hfc interaction with other nuclei. A perusal of the pattern around the 3rd Al hfc component of (H−Al−NH_2):NH_3 shown in Figure 10a suggests that the lower field component of the doublet (due to the H attached to the Al) is masked by the higher field component of the doublet of the insertion radical H−A−NH_2 as indicated. From the difference in the resonance position of the observed third Al hf component of (H−Al−NH_2):NH_3 and that of (D−Al−ND_2):ND_3 (Figure 10a,b), the hfc interaction of the H attached to the Al was assessed as ∼34 G. The *g* value and the Al and the H coupling constants thus determined are given in Table 1.

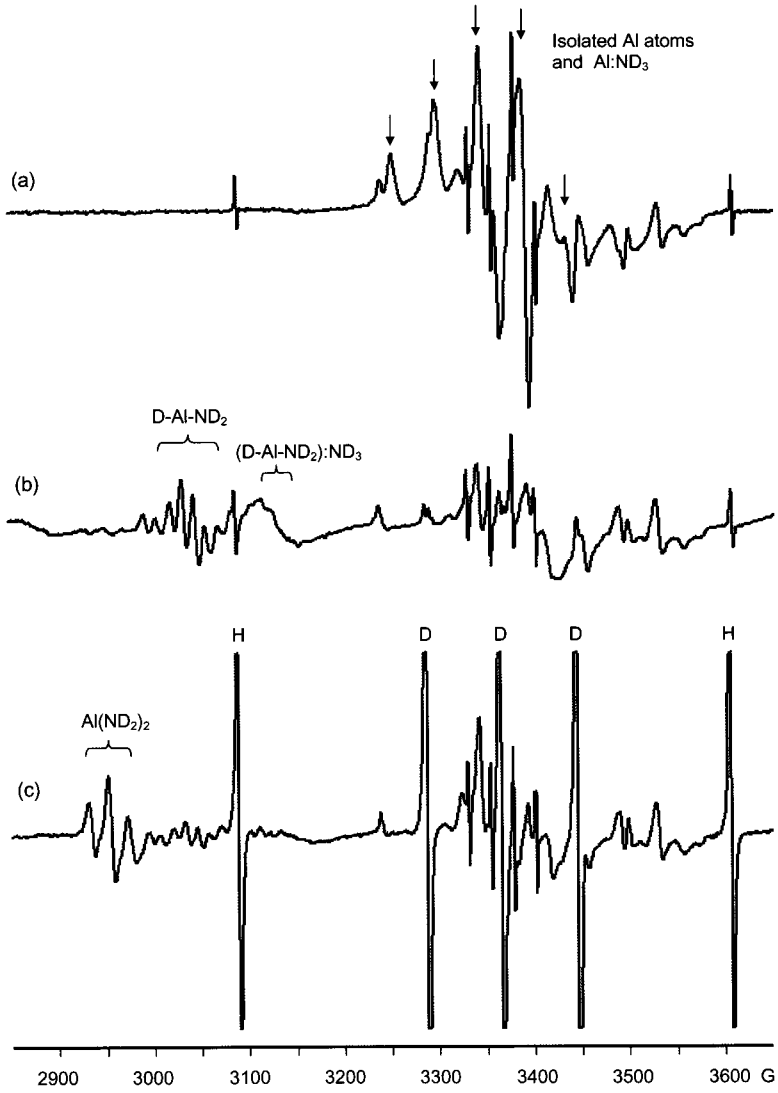

Figure 9. ESR spectra obtained from the same matrix as in Figure 8 scanning the central range: (a) as prepared, (b) after irradiation with near-IR light ($\lambda = 700 \pm 50$ nm) for 20 min, and (c) after subsequent irradiation with blue light ($\lambda = 450 \pm 50$ nm) for 20 min. The arrows in (a) indicate the photolabile signals due to the dative complex Al:ND_3.

TABLE 2: Isotropic and Orientation-Dependent Parts of the Al hfc Tensors, A_{iso} and A_{dip}, Computed from the Observed hfc Tensors[a]

radical	A_{iso} (G)	A_{dip} **(G)**	$\rho(Al_{3s})$	$\rho(Al_{3p})$	$\rho(H_{H-Al})$
Al:NH_3	5	25.7		0.86 (0.99)	
H−Al−NH_2	339	18.3	0.24 (0.34)	0.61 (0.51)	0.15 (0.10)
(H−Al−NH_2):NH_3	278	13.3	0.20 (0.32)	0.44 (0.45)	0.07 (0.07)
Al$(NH_2)_2$	407	11.7	0.29 (0.45)	0.39 (0.42)	

[a] The spin densities in the Al 3s and 3p orbitals thus determined are compared with the values given by the MO theory (in parentheses). The observed and calculated spin densities at the H attached to the Al are also shown.

Analysis of the Spectrum due to Al$(NH_2)_2$. The sextet pattern due to an Al hfc tensor of axial symmetry was readily recognized for the spectrum of Al$(^{15}ND_2)_2$ (Figure 8c). The **g** tensor and the Al hfc tensor of the diligand species Al$(NH_2)_2$ were hence determined as given in Table 1. Figure 11a shows, in an expanded scale, the third Al hf component region of the spectrum due to Al$(^{15}ND_2)_2$ (Figure 8c). The indicated 1:2:1 hf structure clearly attests to the presence of two equivalent ^{15}N ($I = 1/2$) nuclei. As stated earlier, the SOMO of the diligand species predicted an hfc interaction with two amino protons situated trans to the main spin density lobe (cf. Figure 2b). The result obtained above for the insertion radical H−Al−NH_2 has shown that the amino proton (trans to the spin density lobe) has an hfc constant (accidentally) close to that of the ^{14}N hfc constant. The extra complexity observed in the third Al hf component of Al$(NH_2)_2$ (Figure 11b) was thus ascribed to the additional hfc interaction with two protons similar in magnitude to those of the two ^{14}N ($I = 1$) nuclei. Figure 11c shows the computer-simulated pattern based on the **g** and Al hfc tensors determined for Al$(NH_2)_2$ (Table 1) and the additional hfc interactions of 14 G with two ^{14}N nuclei and 10 G with two protons.

Summary and Discussions

The insertion process of the Al atom into the NH_3 molecule was examined by a semiempirical SCF molecular orbital method (AM1) and by matrix isolation ESR spectroscopy. The MO study has revealed that the process would occur in three steps:

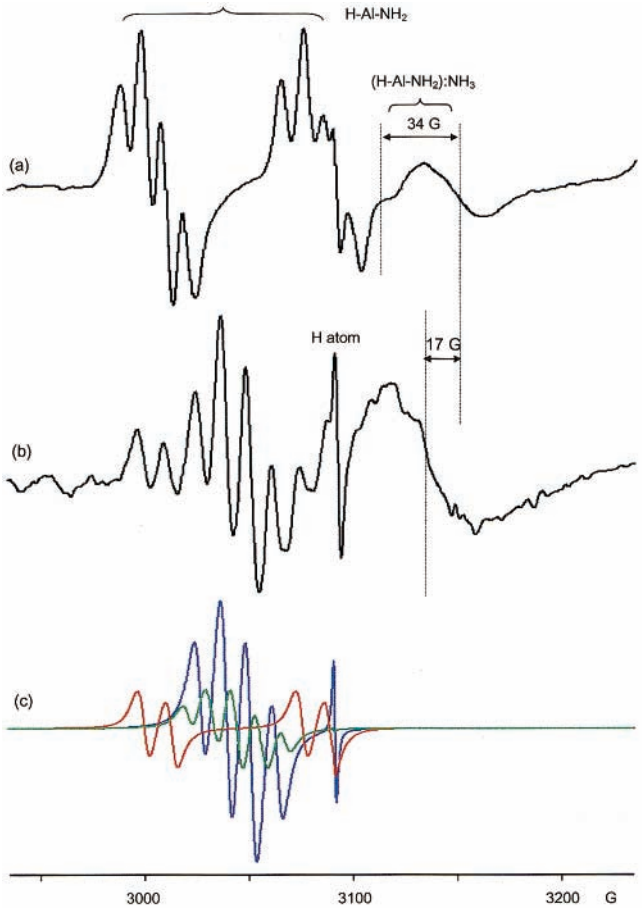

Figure 10. Third Al hf component region of the ESR spectra of the insertion radicals $H-Al-NH_2$ and $(H-Al-NH_2):NH_3$ observed from (a) the Al/NH_3 (1%)/argon system and (b) the $Al/^{15}ND_3$ (2%)/argon system. The lower field component (of the doublet due to the H attached to the Al) of the $(H-Al-NH_2):NH_3$ signal is masked by the higher field component of the $H-Al-NH_2$ signal. (c) Third Al hf component of $D-Al-^{15}ND_2$ (shown in blue), that of $H-Al-^{15}ND_2$ (shown in red), and that of $D-Al-^{15}NDH$ (shown in green) simulated on the basis of the **g** tensor and the hfc tensors given in Table 1 for the assumed abundance ratio of 3/1/1.

(1) spontaneous formation of the dative complex $Al:NH_3$ driven by the three-electron bonding interaction between the unpaired electron of the Al and the lone pair electrons on the N, (2) cleavage of one of the hydrogen atoms upon vibrational excitation (irradiation with near-IR light) of the dative complex, and (3) completion of the insertion process driven by the three-electron bonding interaction between the unpaired electron of the cleaved H and the lone pair electrons on the Al atom. In the dative complex $Al:NH_3$, the unpaired electron resides in a nonbonding Al p orbital perpendicular to the Al−N internuclear direction. The insertion product $H-Al-NH_2$ is planar, and the unpaired electron is localized in the nonbonding Al sp-hybridized orbital in the plane. For $H-Al-NH_2$, in addition to a large hf interaction with the H attached to the Al, the theory predicted a possibly observable hf interaction with the amino proton situated trans to the main spin density lobe.

The matrix isolation ESR study of the Al/NH_3/argon system revealed the presence of the dative complex $Al:NH_3$ spontaneously formed in the original matrix. Subsequent irradiation of the matrix with near-IR light ($\lambda = 700 \pm 50$ nm) resulted in a total disappearance of the dative complex and concurrent formation of the insertion radical $H-Al-NH_2$ in good accord with the process predicted by the MO study. In matrixes with higher NH_3 concentration ($\geq 2\%$), the spectrum due to the insertion radical complexed to the second NH_3 molecule, $(H-Al-NH_2):NH_3$, was also observed.

Most interestingly when these matrixes were further irradiated with blue light ($\lambda = 700 \pm 50$ nm), the signals due to these insertion radicals diminished with concurrent appearance of intense signals due to hydrogen atoms and, in matrixes with a higher NH_3 concentration, the spectrum due to the diligand species $Al(NH_2)_2$. The observed decay of $H-Al-NH_2$ is consistent with the photolysis process $H-Al-NH_2 \rightarrow H\bullet + Al-NH_2$ reported earlier by Himmel et al.[6] The intensity of $Al(NH_2)_2$ was found to parallel that of *the complexd insertion radical* $(H-Al-NH_2):NH_3$ present prior to irradiation. The formation of the diligand species was thus ascribed to the photolysis $(H-Al-NH_2):NH_3 \rightarrow 2H\bullet + Al(NH_2)_2$.

The Al hfc tensors determined for the various radicals observed in the present study are all (basically) axially symmetric (see Table 1). The principal elements of the tensor are thus given by $A_{||} = A_{iso} + 2A_{dip}$ and $A_{\perp} = A_{iso} - A_{dip}$, where A_{iso} is the isotropic component due to the spin density in the Al 3s orbital and A_{dip} is the anisotropic component due to the spin density in the Al 3p orbital.[15] The analysis of the observed Al tensors by these equations yielded the result given in Table 2. The unpaired electron densities in the Al 3s and 3p orbitals may then be deduced by comparison with $A^{\circ}_{iso} = +1400$ G computed for a unit spin density in the Al 3s orbital, and $A^{\circ}_{dip} = +30$ G computed for a unit spin density in the Al 3p orbital.[16] The results are also shown in Table 2. The unpaired electron distributions are also given by the molecular orbital calculations performed above. The values given by the theory are also shown in Table 2 (in parentheses). The large isotropic hfc interactions observed for the H attached to the Al atom in $H-Al-NH_2$ and $(H-Al-NH_2):NH_3$ are due to the spin density in the H 1s orbital. It may be compared with the doublet splitting of the hydrogen atoms generated in the same matrix with an A_{iso} of +505 G. The spin densities in the H attached to the Al thus determined are also shown in Table 2 in comparison with the theoretical values. The agreement between the spin densities determined experimentally and those given by the theory (AM1) are far from perfect. However, the "trend" given by the theory is in good agreement with that observed in each category.

As stated earlier, the hfc tensors of Al atoms isolated in rare gas matrixes had been analyzed by Ammeter et al.[12] The ESR spectra of the otherwise degenerate system ($3s^23p^1$) become observable owing to an axially symmetric lattice distortion. The unpaired electron thus resides in the nondegenerate 3p orbital. The hfc tensor of $A_{||} = +47.7$ G and $A_{\perp} = -33.7$ G has been determined for Al atoms isolated in an argon matrix. These values yield $A_{iso} = -6.6$ G and $A_{dip} = +27.1$ G. The small negative A_{iso} is due to spin polarization of filled s orbitals. The A_{dip} value is close to the computed "atomic value" of 30 G. As stated earlier the MO study showed that the SOMO of the dative complex $Al:NH_3$ is also essentially an Al 3p orbital. The signs of the hfc tensor elements cannot be determined from the spectrum. Let us assume, in line with the tensor concluded for isolated Al atoms, $A_{||} = +47.0$ G and $A_{\perp} = -30.0$ G for the dative complex. One then obtains $A_{iso} = -5$ G and $A_{dip} = +25.7$ G. The A_{dip} value is close to, but slightly smaller than, that of Al atoms isolated in argon, as expected.

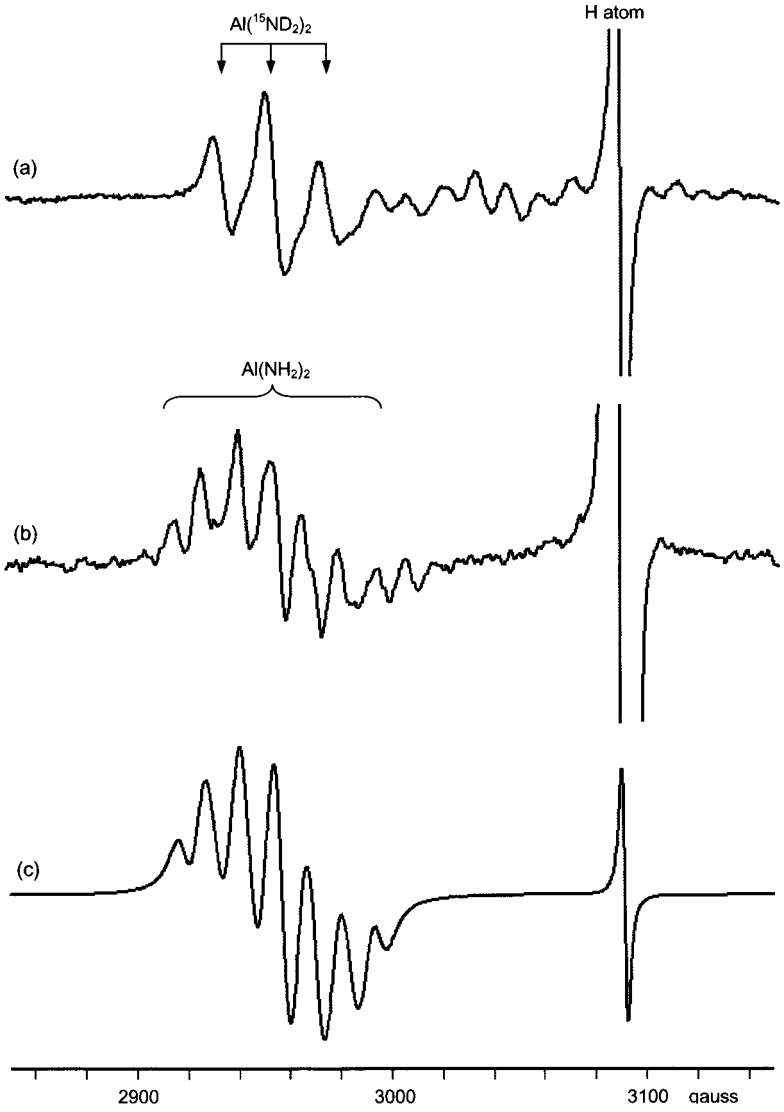

Figure 11. Third Al hf component region of the ESR spectrum of the diligand complex $Al(NH_2)_2$ or $Al(^{15}ND_2)_2$ observed from (a) the $Al/^{15}ND_3$ (2%)/argon system and (b) the Al/NH_3 (1%)/argon system. (c) Third Al hf component of $Al(NH_2)_2$ simulated on the basis of the **g** tensor and the hfc tensors given in Table 1.

References and Notes

(1) Hauge, R. H.; Kauffman, J. W.; Margrave, J. L. *J. Am. Chem. Soc.* **1980**, *102*, 6005.

(2) Knight, L. B., Jr.; Gregory, B.; Cleveland, J.; Arrington, C. A. *Chem. Phys. Lett.* **1993**, *204*, 168.

(3) Howard, J. A.; Joly, H. A.; Edwards, P. P.; Singer, R. J.; Logan, D. E. *J. Am. Chem. Soc.* **1992**, *114*, 474.

(4) Chenier, J. H. B.; Howard, J. A.; Joly, H. A.; LeDuc, M.; Mile, B. *J. Chem. Soc., Faraday Trans.* **1990**, *86*, 3321.

(5) Köppe, R.; Kasai, P. H. *J. Am. Chem. Soc.* **1996**, *118*, 135.

(6) Himmel, H.; Downs, A. J.; Greene, T. M. *J. Am. Chem. Soc.* **2000**, *122*, 2793.

(7) Kasai, P. H. *J. Phys. Chem.*, in press.

(8) Kasai, P. H. *Acc. Chem. Res.* **1971**, *4*, 329.

(9) *HyperChem 5.1*; Hypercube, Inc.: Gainesville, FL., 1998.

(10) Kasai, P. H. *J. Am. Chem. Soc.* **1972**, *94*, 5950.

(11) *Absoft Pro Fortran 5.0*; Absoft Corp.: Rochester Hills, MI, 1998.

(12) Ammeter, J. H.; Schlosnagle, D. C. *J. Chem. Phys.* **1973**, *59*, 4784. For ESR spectra of Al atoms in rare gas matrixes, see: Knight, L. B., Jr.; Weltner, W., Jr. *J. Chem Phys.* **1971**, *55*, 5066.

(13) Himmel et al. To be published.

(14) Kasai, P. H.; McLeod, D., Jr. *Faraday Discuss. Symp. 14, Chem Soc.* **1980**, 65.

(15) See, for example: Smith, W. V.; Sorokin, P. P.; Gelles, I. L.; Lasher, G. J. *Phys. Rev.* **1959**, *115*. 1546.

(16) Morton, J. R.; Preston, K. F. *Magn. Reson.* **1978**, *30*, 577.